

RESEARCH

Open Access



Mechanistic insights of lenvatinib: enhancing cisplatin sensitivity, inducing apoptosis, and suppressing metastasis in bladder cancer cells through EGFR/ERK/P38/NF- κ B signaling inactivation

Chih-Hung Chiang^{1,2,3†}, Jr-Di Yang⁴, Wei-Lin Liu^{5†}, Fang-Yu Chang⁶, Che-Jui Yang⁷, Kai-Wen Hsu^{8,9,10*}, I-Tsang Chiang^{11,12,13} and Fei-Ting Hsu^{6,14*}

Abstract

Background The persistent activation of the epidermal growth factor receptor (EGFR) leads to the activation of downstream oncogenic kinases and transcription factors, resulting in tumor progression and an increased resistance to cisplatin in bladder cancer (BC) cells. Lenvatinib, an oral multikinase inhibitor, has the potential to offer therapeutic benefits as an adjuvant treatment for BC patients. The investigation into its application in bladder cancer treatment is a valuable endeavor. The primary goal of this study is to confirm the effectiveness and mechanism of lenvatinib in inhibiting the progression of BC and enhancing the anticancer efficacy of cisplatin.

Materials Three BC cell lines, namely, TSGH-8301, T24, and MB49, along with an MB49-bearing animal model, were utilized in this study.

Results In vitro experiments utilizing MTT assays demonstrated that lenvatinib sensitized BC cells to cisplatin, exhibiting a synergistic effect. Flow cytometry indicated apoptotic events and signaling, presenting that lenvatinib effectively induced apoptosis and triggered extrinsic/intrinsic apoptotic pathways. In vivo studies using a mouse model of BC confirmed the antitumor efficacy of lenvatinib, demonstrating significant tumor growth suppression without inducing toxicity in normal tissues. Western blotting analysis and immunohistochemistry stain revealed EGF-phosphorylated EGFR and EGFR-mediated ERK/P38/NF- κ B signaling were suppressed by treatment with lenvatinib. In addition, lenvatinib also suppressed anti-apoptotic (MCL1, c-FLIP, and XIAP) and metastasis-related factors (Twist,

[†]Chih-Hung Chiang, and Wei-Lin Liu contributed equally to this work.

*Correspondence:

Kai-Wen Hsu

kwhsu@mail.cmu.edu.tw

Fei-Ting Hsu

sakiro920@gmail.com; sakiro920@mail.cmu.edu.tw

Full list of author information is available at the end of the article



© The Author(s) 2024. **Open Access** This article is licensed under a Creative Commons Attribution-NonCommercial-NoDerivatives 4.0 International License, which permits any non-commercial use, sharing, distribution and reproduction in any medium or format, as long as you give appropriate credit to the original author(s) and the source, provide a link to the Creative Commons licence, and indicate if you modified the licensed material. You do not have permission under this licence to share adapted material derived from this article or parts of it. The images or other third party material in this article are included in the article's Creative Commons licence, unless indicated otherwise in a credit line to the material. If material is not included in the article's Creative Commons licence and your intended use is not permitted by statutory regulation or exceeds the permitted use, you will need to obtain permission directly from the copyright holder. To view a copy of this licence, visit <http://creativecommons.org/licenses/by-nc-nd/4.0/>.

Snail-1, ZEB-1, ZEB-2, and MMP9) and promoted epithelial markers (E-cadherin) while reducing mesenchymal markers (N-cadherin).

Conclusion In conclusion, the induction of apoptosis and the inhibition of EGFR/ERK/P38/NF- κ B signaling are correlated with lenvatinib's ability to hinder tumor progression and enhance the cytotoxic effects of cisplatin in bladder cancer. These findings underscore the potential of lenvatinib as a therapeutic option for bladder cancer, either as a standalone treatment or in combination with cisplatin.

Keywords Lenvatinib, Cisplatin, EGFR, ERK, NF- κ B, Bladder cancer

Introduction

Bladder cancer, which represents the most commonly occurring urothelial carcinoma, exhibits two primary classifications: nonmuscle invasive bladder cancer (NMIBC) and muscle invasive bladder cancer (MIBC) [1]. The efficacy of conventional therapies, including radical cystectomy, chemotherapy, and radiotherapy, is constrained by the high incidence of cancer recurrence and metastasis [2, 3]. The exploration and development of potential adjunctive treatments targeting the reduction of bladder cancer recurrence and metastasis constitute a critical research area with the objective of improving treatment outcomes.

The overexpression of epidermal growth factor receptor (EGFR), a tyrosine kinase transmembrane receptor, contributes to tumor progression and is associated with poor outcomes in bladder cancer [4]. EGFR activates downstream oncogenic pathways to facilitate cell growth, anti-apoptosis, metastasis, angiogenesis, and epithelial-mesenchymal transition (EMT) in cancers [5, 6]. As demonstrated through cell and animal models, it has been proven that EGFR inactivation not only inhibits growth but also increases sensitivity to radiation in bladder cancer [7, 8]. In addition, erlotinib, an EGFR inhibitor, has been demonstrated to provide beneficial effects as a neoadjuvant therapy in bladder cancer patients undergoing radical cystectomy [9].

Lenvatinib is a multikinase inhibitor that elicits tumor regression by targeting oncogenic and angiogenic kinases, including fibroblast growth factor (FGF) receptors, tyrosine-protein kinase KIT (CD117), vascular endothelial growth factor (VEGF) receptors, and platelet-derived growth factor receptor [10]. Our previous studies have demonstrated that lenvatinib suppresses the progression of non-small cell lung cancer (NSCLC) and hepatocellular carcinoma (HCC) by attenuating the AKT, protein kinase C delta (PKC- δ), and mitogen-activated protein kinase (MAPK) signaling pathways [11, 12]. These oncogenic kinases may be involved in EGFR-mediated tumor progression [13–15]. However, it remains ambiguous whether the inhibition of EGFR signaling is implicated in the lenvatinib-triggered suppression of bladder cancer.

Therefore, the primary objective of the current study was to investigate the inhibitory effectiveness of lenvatinib on the EGFR signaling-mediated progression of bladder cancer.

Materials and methods

Chemicals, antibodies and reagents

Lenvatinib, fetal bovine serum (FBS), MTT (3-(4,5-dimethylthiazol-2-yl)-2,5-diphenyltetrazolium bromide), and dimethyl sulfoxide (DMSO) were obtained from Sigma Chemical Co. (St. Louis, MO, USA). Detailed information on the antibodies is listed in Table 1.

Cell culture

The human bladder carcinoma T24 cell line and murine bladder carcinoma MB49 cells were both obtained from the Bioresource Collection and Research Centre (BCRC) in Taiwan. The TSGH-8301 cell line was provided by Professor Jing-Gung Chung's lab at China Medical University. Cells were cultured in McCoy's 5 A medium, RPMI 1640 medium, and DMEM high glucose medium supplemented with 10% fetal bovine serum, 1% penicillin-streptomycin, and L-glutamine. Cells were maintained in culture dishes before each experiment at 37 °C with 5% CO₂ [16].

3-(4,5-dimethylthiazol-2-yl)-2,5-diphenyltetrazoliumbromide (MTT assay)

Cells viability analysis were performed to assess the toxic effects of lenvatinib on the T24, TSGH-8301, and MB49 cell lines. Initially, 5×10^3 cells/well were seeded overnight in 96-well plates. Different concentrations of lenvatinib (0, 5, 10, 20, 30 μ M), cisplatin (0, 1, 2, 3, 4, 5 μ M) or a combination of both were added, and the cells were incubated for 24 and 48 h. The MTT stock solution was prepared using 1 \times PBS at a concentration of 5 mg/ml. After the treatment period, the medium was removed, and 100 μ l of MTT solution (50 mg/mL) (1:9 = MTT stock: medium) was added to each well. The plates were then incubated at 37 °C for 4 h. Subsequently, the MTT solution was aspirated, and 100 μ l of DMSO was added. The signal released from the plates was detected using an ELISA reader (Thermo Fisher

Table 1 The antibodies used in this study are listed as follows:

Primary Antibody	Catalog Number	Host	Company	Dilution
p-ERK (Phospho-p44/42 MAPK (Erk1/2) (Thr202/Tyr204) (D13.14.4E)	#4370	Rabbit mAb	Cell Signaling	1:1000
ERK p44/42 MAPK (Erk1/2) (137F5)	#4695	Rabbit mAb	Cell Signaling	1:1000
p-EGFR (Phospho-EGF Receptor) (Tyr1068) (D7A5)	#2234	Rabbit mAb	Cell signaling	1:1000
EGFR	E-AB-63,555	Rabbit mAb	Elabscience	1:1000
p-p38 MAPK (Phospho-p38 MAPK (Thr180/Tyr182) (D3F9)	#4511	Rabbit mAb	Cell signaling	1:1000
p38 MAPK	#9212	Rabbit mAb	Cell signaling	1:1000
p-NF-κB (Phospho-NF-κB p65 (Ser536) (93H1)	#3033	Rabbit mAb	Cell signaling	1:1000
NF-κB p65 (D14E12)	#8242	Rabbit mAb	Cell signaling	1:1000
VEGFA (vascular endothelial growth factor)	ab1316	Mouse mAb	Abcam	1:5000
MCL-1 (myeloid cell leukemia-1)	E-AB-33,430	Rabbit mAb	Elabscience	1:1000
MMP9 (matrix metalloproteinase9)	E-AB-63,483	Rabbit mAb	Elabscience	1:500
XIAP (X-linked inhibitor of apoptosis protein (XIAP)	PA5-29253	Rabbit mAb	Thermo Fisher Scientific	1:1000
c-FLIP (cellular FLICE-like inhibitory protein)	(E-AB-14081)	Rabbit mAb	Elabscience	1:1000
Twist (TWIST1)	#46,702	Rabbit mAb	Cell signaling	1:1000
Snail-1 (C15D3)	#3879	Rabbit mAb	Cell signaling	1:1000
N-Cadherin	#13,116,	Rabbit mAb	Cell signaling	1:1000
E-Cadherin	#3195	Rabbit mAb	Cell signaling	1:500
ZEB-1 (E2G6Y)	#70,512	Rabbit mAb	Cell signaling	1:1000
ZEB-2 (E6U7Z)	#97,885	Rabbit mAb	Cell signaling	1:1000
β-actin	E-AB-20,058	Rabbit mAb	Elabscience	1:2000
GAPDH	CSB-PA00025A0Rb	Rabbit mAb	CUSABIO Biotech	1:1000
Vinculin	PA5-29688	Rabbit mAb	Invitrogen	1:1000

Scientific, Fremont, CA, USA). The absorption wavelength for MTT detection was 570 nm [17].

NF-κB plasmid transfection and stable clone selection

An NF-κB reporter gene system was established in TSGH-8301 cells using a plasmid obtained from Promega (Madison, WI, USA). Transfection was performed using the JetPEI™ transfection agent (Illkirch, Bas-Rhin, France). A total of 2×10^5 cells were seeded in a 6 cm Petri dish and incubated overnight. A DNA complex was formed by adding 2 μL of jetPEI™ solution (mixed with 98 μL of NaCl) to 100 μL of DNA solution containing 2 μg of p-NF-κB/luc2, followed by incubation at room temperature for 20 min. After transfection, cells were treated with G418 at a concentration of 50 mg/ml for stable clone selection. NF-κB activation in TSGH-8301 cells was detected using the IVIS Lumina LT Series II imaging system (PerkinElmer, Boston, MA, USA). Cells exhibiting a stable luc2 signal were designated TSGH-8301/NF-κB/luc2 cells [18, 19].

NF-κB reporter gene assay

TSGH-8301/NF-κB/luc2 cells were seeded overnight in a 96-well plate at a density of 5×10^3 cells per well. The cells were then treated with different concentrations (0, 10, 20 μM) of lenvatinib, 0.5 μM NF-κB inhibitor (QNZ), 10 μM ERK inhibitor (PD98059), 10 μM AKT inhibitor (LY294002), 10 μM EGFR inhibitor (erlotinib) and 10 μM P38 inhibitor (SB203580) for

48 h. After 24 h of treatment, a D-luciferin solution (500 μM D-luciferin in 100 μL of 1×PBS) was added to each well and incubated for 15 min. The cells were then imaged using an IVIS 200 system for three minutes, and the activation of NF-κB was normalized to cell viability obtained from the MTT assay [20].

Cell cycle analysis

T24 and TSGH-8301 cells were seeded overnight in a 6-well plate at a density of 2×10^5 cells per well. The cells were then treated with different concentrations (0, 10, and 20 μM) of lenvatinib for 48 h. After the treatment period, the cells were collected by centrifugation, fixed with 75% ethanol, and stored overnight at -20 °C. Following that, the cells were washed with 1×PBS, centrifuged, and stained with a propidium iodide (PI) dye solution (containing PI at a concentration of 40 μg/ml, 100 μg/ml RNase, and 1% Triton X-100 in 1×PBS) for one hour at 37 °C in the dark. The signal intensity of the PI dye in T24 and TSGH-8301 cells was then verified using flow cytometry (FACS) (BD Biosciences, FACS Calibur, San, CA, USA) and quantified using FlowJo software [21].

Annexin V/PI double staining

Initially, T24 and TSGH-8301 cells were seeded overnight in a 6-well plate at a density of 2×10^5 cells per well. Subsequently, the cells were treated with different concentrations (0, 10, and 20 μM) of lenvatinib

for 48 h. After the treatment period, the cells were collected by centrifugation and washed with $1\times$ PBS. The collected cells were then resuspended in $100\ \mu\text{l}$ of $1\times$ binding buffer, which contained $5\ \mu\text{l}$ of Annexin V-FITC (FL-1 channel) and $5\ \mu\text{l}$ of PI (FL-2 channel). Following a 10-minute incubation at room temperature in the absence of light, the signal intensity of Annexin V-FITC and PI-PE dyes on T24 and TSGH-8301 cells was analyzed using flow cytometry, and the data were quantified using FlowJo software [17].

Cleaved-caspase-3, 8, 9, FAS-L/FAS activation analysis

T24 and TSGH-8301 cells were seeded in a 6-well plate overnight at a density of 2×10^5 cells per well. The cells were then treated with different concentrations (0, 10, and $20\ \mu\text{M}$) of lenvatinib for 48 h. After the treatment period, the cells were collected by centrifugation and stained with specific caspase activity probes. Caspase-3 activity was assessed using FITC-DEVE-FMK ($5\ \mu\text{l}$ in $1\ \text{ml}$ $1\times$ PBS), caspase-8 activity with RED-IETD-FMK ($5\ \mu\text{l}$ in $1\ \text{ml}$ $1\times$ PBS), and caspase-9 activity with FITC-LEHD-FMK ($5\ \mu\text{l}$ in $1\ \text{ml}$ $1\times$ PBS). The staining was carried out for 30 min in a $37\ ^\circ\text{C}$ incubator. Additionally, FAS staining was performed using FITC-FAS ($5\ \mu\text{l}$ in $1\ \text{ml}$ $1\times$ PBS), and FAS-L staining was performed with PE-FAS-L ($5\ \mu\text{l}$ in $1\ \text{ml}$ $1\times$ PBS). For both FAS and FAS-L staining, cells were placed on ice with the respective dye for 30 min protected from light. Finally, the stained cells were analyzed using flow cytometry, and the data were quantified using FlowJo software [17].

Detecting the loss of mitochondrial membrane potential (MMP)

T24 and TSGH-8301 cells were seeded in a 6-well plate at a density of 2×10^5 cells per well and incubated overnight. The cells were then treated with different concentrations (0, 10, and $20\ \mu\text{M}$) of lenvatinib for 48 h. After the treatment period, the cells were collected by centrifugation, and the mitochondrial membrane potential (MMP) loss was assessed using the DIOC₆ (3,3'-dihexyloxycarbocyanine iodide) staining assay. The cells were stained with $0.1\ \mu\text{M}$ DIOC₆ dye in $1\times$ PBS and incubated at $37\ ^\circ\text{C}$ in the dark. The loss of MMP was measured using flow cytometry, and the data were quantified using FlowJo software [21].

Migration and Invasion assay

T24 and TSGH-8301 cells were seeded at a density of 5×10^5 cells in a 10 cm Petri dish and incubated overnight. The cells were then treated with different concentrations (0, 10, and $20\ \mu\text{M}$) of lenvatinib for 48 h. To assess invasion and migration, transwell inserts with $8\ \mu\text{m}$ pore size were used, either coated with or

without Matrigel (3:7 = Matrigel: medium). After the treatment period, cells were collected and added to the upper chamber at a density of 1×10^5 cells in medium without serum for migration and invasion assays, and the bottom chamber was supplemented with 10% FBS. Transwell membranes were fixed with a fixation buffer (3:1 methanol and acetic acid) for 15 min and stained with 0.01% crystal violet for 10 min. The membranes were then imaged using an optical microscope (Nikon ECLIPSE Ti-U) at $\times 100$ magnification. The number of invaded and migrated cells was quantified using ImageJ software version 1.50 (National Institutes of Health, Bethesda, MD, USA) [22, 23].

Immunofluorescence nuclear translocation

T24 and TSGH-8301 cells were seeded at a density of 5×10^3 cells on a chamber slide overnight and then treated with different concentrations (0, 10, and $20\ \mu\text{M}$) of lenvatinib for 48 h. After the treatment period, the chamber slide was fixed with 4% paraformaldehyde for 15 min. Cells were permeabilized using 0.01% Triton-X100 for 10 min and then blocked with blocking buffer (Axel Biotechnology Inc.) for one hour at room temperature. The slices were incubated overnight at 4 degrees Celsius with the primary antibody (1:350 NF- κ B p65). After antibody incubation, the chamber slide was washed once with PBS-T ($1\times$ PBS with 0.1% Tween 20) and washed twice with $1\times$ PBS. The slices were then incubated with FITC-labeled secondary antibody (Jackson ImmunoResearch Laboratories Inc.) at room temperature for 1 h in the dark. Finally, the slide was mounted with DAPI Fluoromount-G dye, and the fluorescence signal of NF- κ B was observed using a fluorescence microscope (Leica) [21].

Western blotting

T24 and TSGH-8301 cells were seeded at a density of 5×10^5 cells in a 10 cm Petri dish. After overnight incubation, the cells were treated with different concentrations (0, 10, and $20\ \mu\text{M}$) of lenvatinib for 48 h. Following the treatment, proteins were extracted from each group using lysis buffer (Tris-HCl pH 8.0, 120 mM NaCl, 0.5% Nonidet P-40, and 1 mM tosyl sulfonyl fluoride). The total protein concentration was determined using the Pierce BCA Protein Assay Kit (Thermo Fisher Scientific). Protein samples were then separated by 6–12% SDS-PAGE and transferred onto a PVDF membrane. After transfer, the membranes were blocked with blocking buffer and incubated overnight at 4 degrees Celsius with specific primary antibodies as listed in Table 1. The immunodetected proteins on the membranes were visualized using the UVP Chemi-Doc-It™ system (AnalytikJena Jena, Germany), and the band intensities were quantified using Vision Works

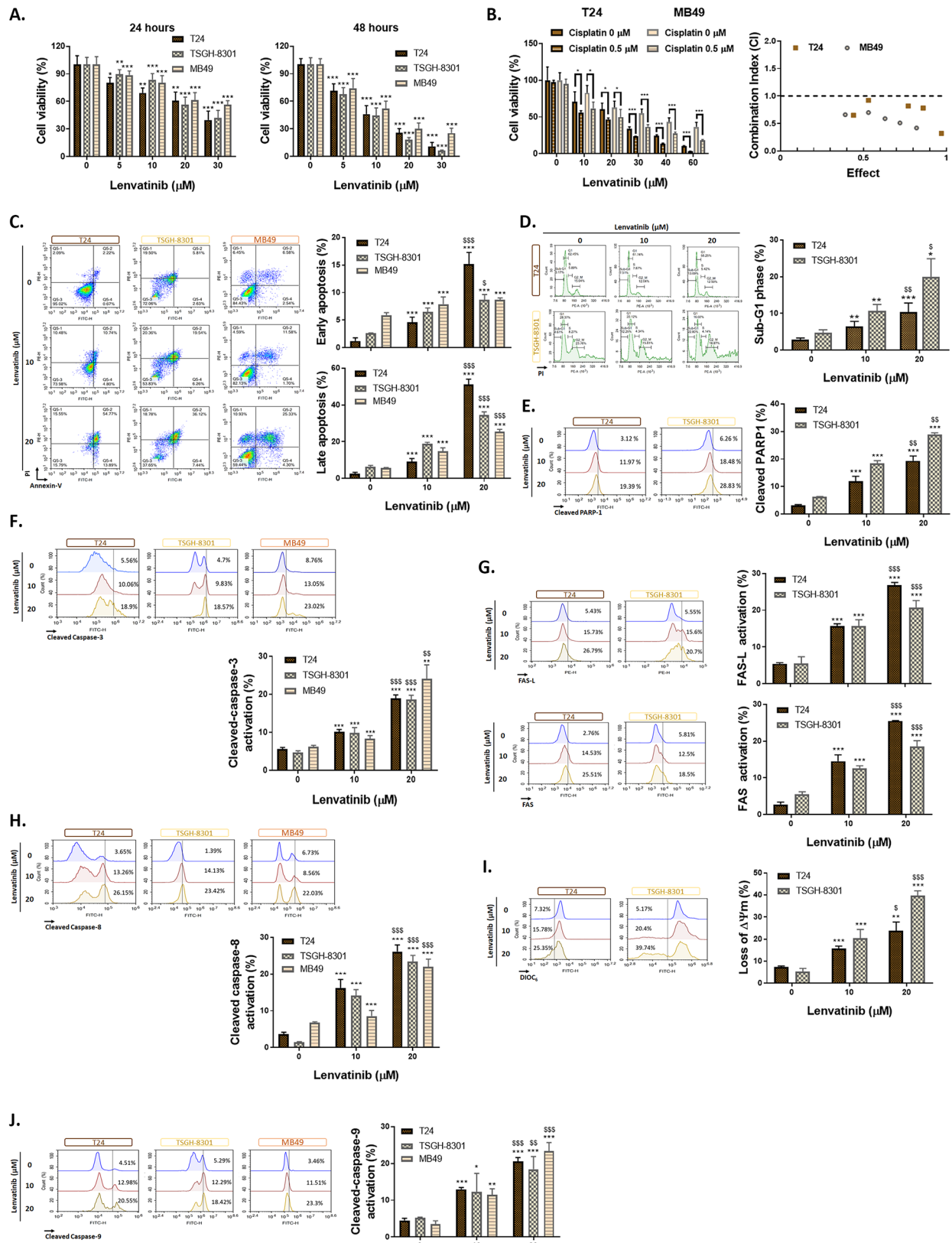


Fig. 1 (See legend on next page.)

(See figure on previous page.)

Fig. 1 Cytotoxicity and apoptosis induction of lenvatinib in BC cells. **(A)** The MTT assay was performed to evaluate the effects of lenvatinib treatment alone for 24 and 48 h. **(B)** The MTT assay was conducted to assess the combination of lenvatinib with cisplatin, and the combination index (CI) was determined. **(C)** Annexin-V/PI staining, **(D)** PI cell cycle analysis, **(E)** cleaved PARP-1 staining and **(F)** cleaved caspase 3 staining after lenvatinib treatment of BC cells were evaluated by flow cytometry. **(G-H)** Flow cytometry was utilized to evaluate FAS, FAS-L, and cleaved caspase-8 staining after lenvatinib treatment of BC cells. **(I-J)** Mitochondrial potential staining (DIOC₆) and cleaved caspase-8 staining after lenvatinib treatment of BC cells were evaluated by flow cytometry. [(*, **, ***) represent statistical significance with *P* values of less than 0.05, 0.01, and 0.0005, respectively, compared to 0 μM lenvatinib. (°, °°, °°°) represent statistical significance with *P* values of less than 0.05, 0.01, and 0.0005, respectively, compared to 10 μM lenvatinib.]

software (Analytik Jena, Jena, Germany). The quantitative data were normalized to β-actin, GAPDH, and vinculin expression and averaged from three independent replicate experiments [24, 25].

Animal experiment

The animal experiment research conducted in this study was approved by the Animal Care and Use Committee at China Medical University (Approval ID: CMU-IACUC-2023-051). Male C57BL/6JNarl mice, six weeks old, were obtained from the National Animal Center and housed at the Animal Center of China Medical University [24].

Animal subcutaneous tumor xenotransplantation

To establish the tumor model, a total of 2×10^6 MB49 cells were subcutaneously implanted into the right flank of the mice [26]. Once the calculated tumor size reached 100 mm^3 (tumor length \times tumor width² $\times 0.523$), the mice were divided into three groups: vehicle (1% DMSO) and lenvatinib treatment at doses of 5 mg/kg and 10 mg/kg. The weight of the mice was recorded twice a week throughout the experiment. On the 11th day after the initiation of lenvatinib treatment, the mice were euthanized, and the tumors were harvested for further analysis [24]. For combination treatment, mice were divided into four groups: untreated control (0.1% DMSO, CTRL), lenvatinib at 5 mg/kg/day/gavage, cisplatin 3 mg/kg/day/ip and combination for a duration of 14 days.

Hematoxylin and eosin (H&E) and immunohistochemistry (IHC) staining

The tumor, heart, liver, kidney, pancreas, intestine, and spleen samples from the mice were fixed and sliced for H&E or IHC staining. For H&E staining, the tumor tissue sections were deparaffinized in diphenylmethyl and rehydrated with a reduced concentration of ethanol. Subsequently, the slides were treated with 3% H₂O₂ for 10 min and washed. To block nonspecific binding, the slides were incubated in 5% normal goat serum in a sealed container for 5 min. The primary antibody was then applied to the slides and incubated overnight at 4 °C. The slides were further incubated with a biotinylated secondary antibody at room temperature for 30 min, followed by counterstaining with hematoxylin. The H&E- and IHC-stained slices were

imaged using a TissueFAXS Tissue Gnostics Axio Observer Z1 microscope (TissueGnostics GmbH). A total of 9 views from each group were quantified using the IHC toolbox in ImageJ software [24, 27].

Statistics analysis

The significant difference between the treatment group and the control group was calculated using Student's *t* test and one-way ANOVA. The statistical analyses were conducted using GraphPad Prism 7 software. All data are presented as the mean \pm standard deviation. A *P* value less than 0.05 was considered statistically significant. Each experiment was replicated three times independently [21].

Results

Toxicity evaluation of lenvatinib on bladder cancer cells (BC) and its potential synergistic effect with cisplatin

To assess the toxicity of lenvatinib on bladder cancer (BC), we conducted an MTT assay on three BC cell lines: TSGH-8301, T24, and MB49. As shown in Fig. 1A, lenvatinib exhibited cytotoxic effects on BC cells in a dose- and time-dependent manner. Table 2 demonstrates the IC₅₀ values of lenvatinib in BC cells after 48 h, ranging from 10 to 13 μM. Additionally, we discovered that lenvatinib has the potential to be combined with the standard treatment cisplatin for further clinical applications. Our combination data from the MTT assay indicated that lenvatinib may sensitize BC cells to cisplatin (Fig. 1B). Compared to the viability observed with a solo treatment of 1 μM cisplatin, which was approximately 95%, the viability decreased to 60% when half the dose of cisplatin was combined with lenvatinib (Supplementary Fig. 1). The synergistic effect (CI < 1) was observed in Fig. 1C, starting from a lenvatinib dosage of 10 μM combined with 2 μM cisplatin.

To further understand how lenvatinib induces toxicity in BC, we examined the apoptotic response. Figure 1C confirmed that lenvatinib induces the accumulation of early and late apoptotic populations in BC cells. The subG1 population, which represents apoptotic cells, also increased following lenvatinib treatment (Fig. 1D). Moreover, the cleaved form of PARP-1, a marker of apoptosis, was effectively triggered by lenvatinib (Fig. 1E). Cleaved caspase-3, an overall caspase-dependent marker, was also found to be

Table 2 The 50% and 70% inhibitory concentrations of lenvatinib after 48 h of treatment in bladder cancer cells

Condition	T24	TSGH	MB49
IC ₅₀	13.41 μ M	10.65 μ M	12.83 μ M
IC ₇₀	19.24 μ M	15.68 μ M	18.65 μ M

increased by lenvatinib (Fig. 1F). Next, we investigated the activity of two potential caspase-dependent apoptotic signaling pathways: the death receptor pathway and the mitochondria-dependent pathway. As depicted in Fig. 1G-H, lenvatinib activated both the death receptor pathway (FAS and its ligand) and the downstream factor caspase-8. Simultaneously, lenvatinib triggered mitochondria-dependent factors, such as the loss of mitochondrial membrane potential ($\Delta\Psi_m$) and caspase-9 activation (Fig. 1I-J). In conclusion, lenvatinib can induce apoptosis mechanisms in BC, thereby enhancing the toxic effect of cisplatin. These findings suggest the potential of lenvatinib as a therapeutic option in combination with cisplatin for BC treatment.

Investigating the oncogene pattern and inhibition of EGFR/ERK/P38/NF- κ B signaling by lenvatinib in bladder cancer cells

To gain insights into the oncogene pattern in BC cells, we conducted Western blotting analysis. As shown in Fig. 2A, NF- κ B was found to be elevated in tumor cells (T24 and TSGH-8301) but not in normal cells (SV-HUC-1, human urinary tract epithelial cells). We also confirmed that NF- κ B activation occurred in a dose-dependent manner after cisplatin treatment in TSGH-8301/NF- κ B-*luc2* cells (Fig. 2B). To overcome the overexpression of NF- κ B in BC cells, we tested various potential inhibitors and lenvatinib using an NF- κ B reporter gene assay. Figure 2C demonstrates that lenvatinib, erlotinib (EGFR inhibitor), PD98059 (ERK inhibitor), and SB20580 (P38 inhibitor) could regulate NF- κ B activation in TSGH-8301/NF- κ B-*luc2* cells. Therefore, whether these inhibitors and drugs have the potential to overcome cisplatin-induced EGFR/NF- κ B activation was also validated. As shown in Fig. 2D-E, lenvatinib effectively suppressed the phosphorylation of EGFR and NF- κ B induced by cisplatin. Furthermore, additional EGF-mediated EGFR activation was used as a positive control to confirm the inhibitory efficacy of lenvatinib on EGFR (Fig. 2F) in three BC cell lines. The activation of EGFR signaling can trigger the nuclear translocation of NF- κ B, which was also blocked by lenvatinib (Fig. 2G). Moreover, lenvatinib reduced the phosphorylation of downstream proteins in the EGFR pathway induced by EGF, including ERK, P38, and NF- κ B (Fig. 2H and supplementary Fig. 2A). The inhibitory effect of lenvatinib on these factors was dose-dependent (Fig. 2I and supplementary Fig. 2B).

The effect of an ERK inhibitor and an NF- κ B inhibitor on these proteins was also confirmed and used as a positive control to elucidate the relationship between these factors (Fig. 2J and supplementary Fig. 2C-D). In summary, lenvatinib may suppresses EGFR/ERK/P38/NF- κ B signaling, and this effect can be maintained under cisplatin or EGF stimulation. These findings highlight the potential of lenvatinib as a promising therapeutic agent for inhibiting the activation of multiple signaling pathways in BC cells.

Investigating the potential antitumor regulation of metastasis and anti-apoptosis-related factors in bladder cancer cells by lenvatinib

To understand how lenvatinib regulates the antitumor effect in BC cells, we evaluated two key aspects of tumor progression: metastasis and anti-apoptosis. As shown in Fig. 3A-C, lenvatinib effectively suppressed the invasion and migration abilities of BC cells. Additionally, epithelial mesenchymal transition (EMT) is a critical process during cancer metastasis, so we investigated the effect of lenvatinib on EMT-related factors [28, 29]. Figure 3D-E demonstrates that Twist, Snail-1, ZEB-1, and ZEB-2 were all decreased in a dose-dependent manner by lenvatinib. Importantly, lenvatinib induced the expression of the epithelial marker E-cadherin while decreasing the expression of the mesenchymal marker N-cadherin (Fig. 3D, F). The metastasis factor MMP9 was also reduced by lenvatinib (Fig. 3D). Moreover, lenvatinib exhibited the ability to suppress the anti-apoptotic effects in BC cells. Figure 3G illustrates that lenvatinib effectively suppressed the expression of antiapoptotic factors such as MCL-1, c-FLIP, and XIAP [30]. In summary, lenvatinib suppresses the progression of BC by inhibiting tumor metastasis and counteracting anti-apoptotic mechanisms. These findings suggest that lenvatinib has potential as a therapeutic agent for targeting both metastatic processes and anti-apoptotic pathways in BC.

Validation of lenvatinib and its combination with cisplatin in suppressing BC progression without inducing normal tissue toxicity in in vivo models

To assess the efficacy of lenvatinib on in vivo subjects, we conducted an animal experiment as depicted in Fig. 4A. Mice were divided into three groups: untreated control (0.1% DMSO, CTRL), lenvatinib at 5 mg/kg/day, and lenvatinib at 10 mg/kg/day for a duration of 11 days. Tumor volume measurements revealed that the tumor suppression effect was significantly enhanced with increasing doses of lenvatinib (Fig. 4B). Additionally, Table 3 presents the significant differences between the untreated and treated groups at different time points. The tumor progression patterns for

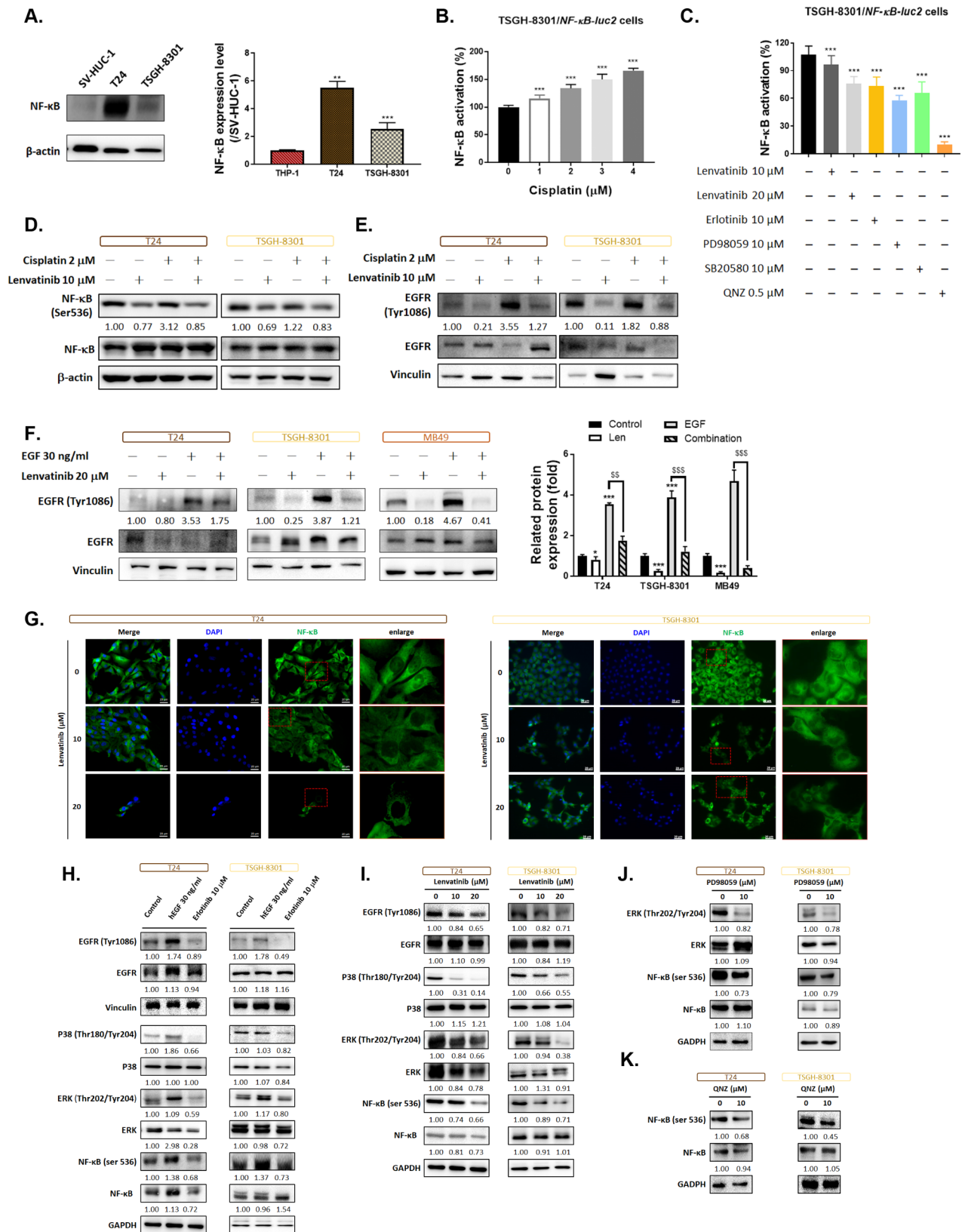


Fig. 2 (See legend on next page.)

(See figure on previous page.)

Fig. 2 Evaluation of the anti-BC mechanism of lenvatinib in BC cells. **(A)** The protein expression of NF- κ B in SV-HUC-1, T24 and TSGH-8301 cells was validated by Western blotting. The activation of NF- κ B after **(B)** cisplatin, **(C)** Lenvatinib, Erlotinib, PD98059 (ERK inhibitor), SB20580 (P38 inhibitor) and QNZ (NF- κ B inhibitor) treatment was performed by reporter gene assay on TSGH-8301/NF- κ B-*luc2* cells. The phosphorylation of NF- κ B and EGFR after **(D-E)** Lenvatinib or **(F)** EGF combined with cisplatin was validated by Western blotting. **(G)** The nuclear translocation of NF- κ B after lenvatinib treatment was visualized using a fluorescence microscope. **(H-K)** Protein expression under different treatment conditions was evaluated using Western blotting. [*****, *******] represent statistical significance with *P* values of less than 0.05 and 0.0005, respectively, compared to 0 μ M lenvatinib. ([§], ^{§§}) represent statistical significance with a *P* value of less than 0.01 and 0.0005 compared to 10 μ M lenvatinib.]

each mouse under different treatment conditions are displayed in Fig. 4C. Lenvatinib effectively prolonged the mean tumor growth time in the MB-49-bearing mouse model (Table 4). Compared to the untreated control group, the delay in tumor progression was 9.28 days for lenvatinib at 5 mg/kg and 23.73 days for lenvatinib at 10 mg/kg. Furthermore, the tumor inhibition rate was 2.46 days for lenvatinib at 5 mg/kg and 4.74 days for lenvatinib at 10 mg/kg. Figure 4D-E show the imaging and weight measurements of the extracted tumors, demonstrating the efficacy of lenvatinib treatment. The lenvatinib-treated group exhibited smaller and lighter tumors. After confirming the treatment efficacy of lenvatinib, we proceeded to evaluate its general toxicity through measurements of body weight, biochemical analysis, and tissue pathology. Figure 4F indicates that the body weight of the mice remained unchanged throughout the entire treatment process. The biochemical markers representing liver function, such as aspartate amino transferase (AST), alanine amino transferase (ALT), and gamma glutamyl transpeptidase (γ GT) values, displayed no significant changes among all the groups (Fig. 4G; Table 5). Moreover, there were no noticeable pathological changes observed in the heart, kidney, liver, spleen, intestine, or pancreas tissues of the mice (Fig. 4H). Furthermore, we confirmed that the therapeutic efficacy of cisplatin may be enhanced by lenvatinib, as shown in Supplementary Fig. 3A. Mice were divided into four groups: untreated control (0.1% DMSO, CTRL), lenvatinib at 5 mg/kg/day, cisplatin 3 mg/kg/day and combination for a duration of 14 days. Superior tumor inhibition was observed with the combination of lenvatinib and cisplatin (Supplementary Fig. 3B-C). Body weight and normal tissue pathology, including the heart, liver, spleen, lungs, kidneys, and intestines, showed no significant changes after treatment, demonstrating the safety of the treatment (Supplementary Fig. 3D-E). In conclusion, the antitumor efficacy and safety of lenvatinib were confirmed in the MB-49-bearing mouse model.

Validation of apoptosis induction and EGFR/ERK/P38/NF- κ B signaling inactivation by lenvatinib in an in vivo BC model

To determine whether the apoptosis induction and inactivation of the EGFR/ERK/P38/NF- κ B signaling

pathway observed in vitro can also be replicated in an in vivo model, we conducted further validation. Figure 5A and C demonstrate that Lenvatinib treatment induced the activation of caspase-3, -8, and -9, key regulators of apoptosis. Conversely, the expression of antiapoptotic factors, such as MCL-1, c-FLIP, and XIAP, was suppressed upon lenvatinib administration (Fig. 5B-C). Furthermore, lenvatinib exhibited inhibitory effects on the metastasis factor MMP9 (Fig. 5B-C). In tumor tissue, lenvatinib was also found to suppress EMT-related factors, including Twist, Snail-1, ZEB-1, and ZEB-2 (Fig. 5D, F). Lenvatinib increased the expression of E-cadherin while decreasing the expression of N-cadherin, thus counteracting the effects of EMT in breast cancer (Fig. 5E, F). The phosphorylation of EGFR, ERK, P38, and NF- κ B was significantly suppressed by lenvatinib in a dose-dependent manner (Fig. 5G). In conclusion, Lenvatinib effectively induces apoptosis and inhibits BC progression by inactivating the EGFR/ERK/P38/NF- κ B signaling pathways (Fig. 6).

Discussion

EGFR overexpression is significantly correlated with muscle invasion and recurrence of bladder cancer [31]. Activation of EGFR is initiated by its ligands, such as EGF and transforming growth factor alpha (TGF α), leading to the promotion of tumor progression through downstream oncogenic pathways. NF- κ B is a pivotal oncogenic diver involved in EGFR-mediated tumor growth, survival, and metastasis [5, 32–34]. Several studies have provided evidence that mitogen-activated protein kinases (MAPKs), such as ERK and P38, play roles in the regulation of NF- κ B activation in bladder cancer [19, 35]. Our data revealed that EGF positively regulates the activation of EGFR/ERK/P38/NF- κ B signaling, while both erlotinib and lenvatinib exert a negative regulatory effect on this signaling pathway (Figs. 2H-I and 5G). Importantly, lenvatinib also significantly downregulated EGFR phosphorylation at the Tyr1086 site induced by EGF (Fig. 2F). These findings suggest that lenvatinib inactivates EGFR, thereby attenuating the ERK/P38/NF- κ B signaling pathway.

Cisplatin, an alkylating agent, is utilized as the primary chemotherapy option for metastatic bladder cancer, but its effectiveness is diminished by EGFR/NF- κ B signaling. Cisplatin has been shown to induce

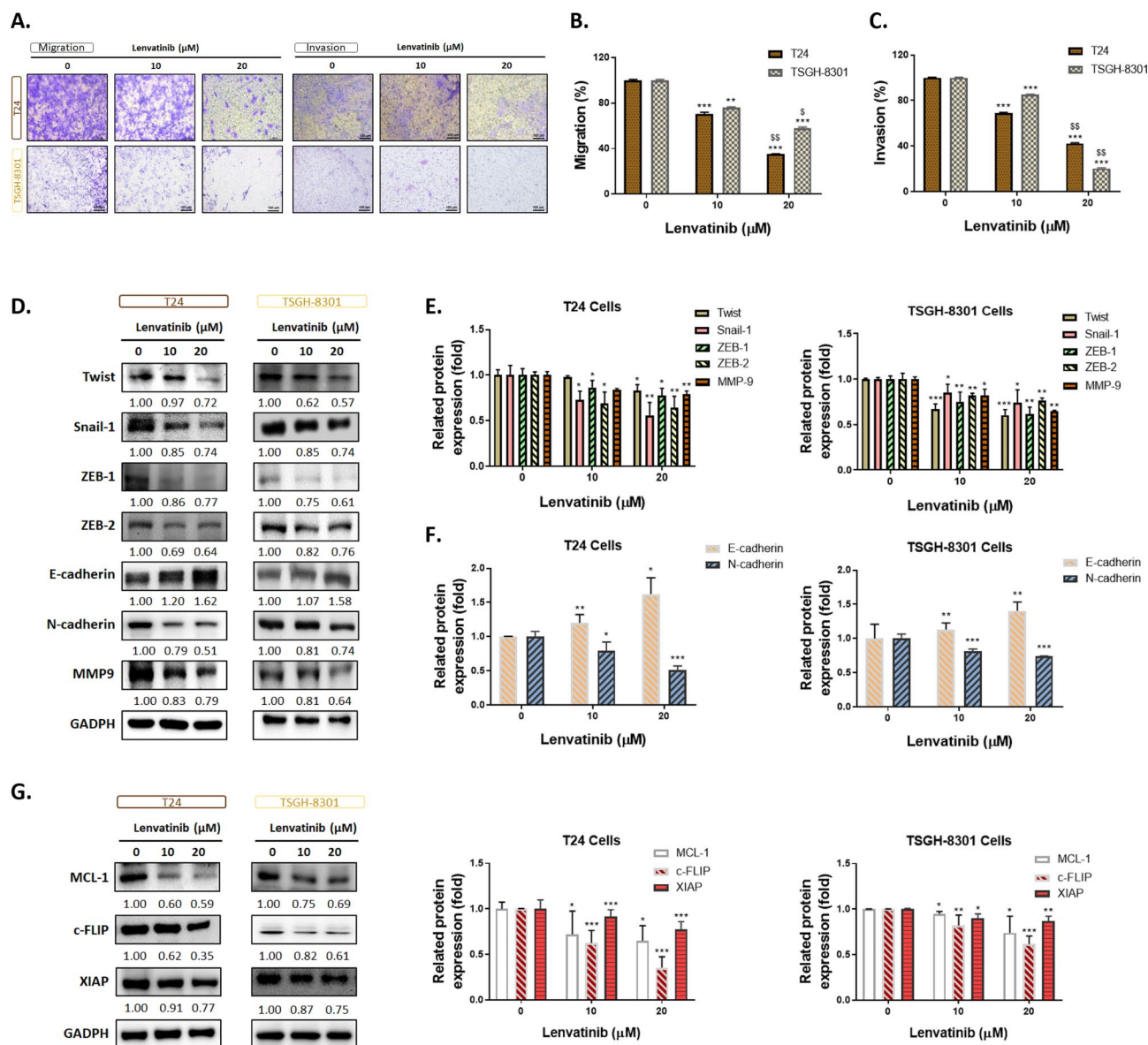


Fig. 3 Metastatic and antiapoptotic effects of lenvatinib on BC cells. **(A)** The invasion/migration patterns of T24 and TSGH-8301 cells were observed after lenvatinib treatment, and the results are presented. **(B-C)** Quantification of the invasion/migration data for T24 and TSGH-8301 cells after lenvatinib treatment is provided. **(D)** The protein expression patterns of Twist, Snail-1, ZEB-1, ZEB-2, MMP9, E-cadherin and N-cadherin were determined by Western blotting, and **(E-F)** their quantification results are presented. **(G)** The protein expression patterns of MCL-1, c-FLIP and XIAP determined by Western blotting and their quantification results are presented. [(*, **, ***) represent statistical significance with P values of less than 0.05, 0.01, and 0.0005, respectively, compared to 0 μM lenvatinib.]

cytotoxicity while also activating EGFR/NF- κB signaling in bladder cancer [36, 37]. Lenvatinib may also sensitize BC to cisplatin treatment (Supplementary Fig. 3). In the present study, we also observed similar findings. Notably, lenvatinib not only inhibited the activation of EGFR/NF- κB by cisplatin but also effectively sensitized bladder cancer cells to cisplatin (Figs. 1B and 2B 2D-E). MCL-1, c-FLIP, and XIAP act as anti-apoptotic mediators, and their expression is linked to the constitutive activation of NF- κB . The reduction in anti-apoptotic proteins enhances the anticancer efficacy of

cisplatin [26, 38]. Our data indicated that treatment with lenvatinib significantly reduced the protein levels of MCL-1, c-FLIP, and XIAP in bladder cancer both in vitro and in vivo. (Figures 3G and 5B). Suppression of EGFR/NF- κB signaling may contribute to the synergistic growth inhibitory efficacy of the combined treatment of lenvatinib with cisplatin in bladder cancer cells.

The importance of an anticancer drug has both the ability to induce apoptosis in cancer cells and the ability to inhibit the mechanisms that protect cancer cells

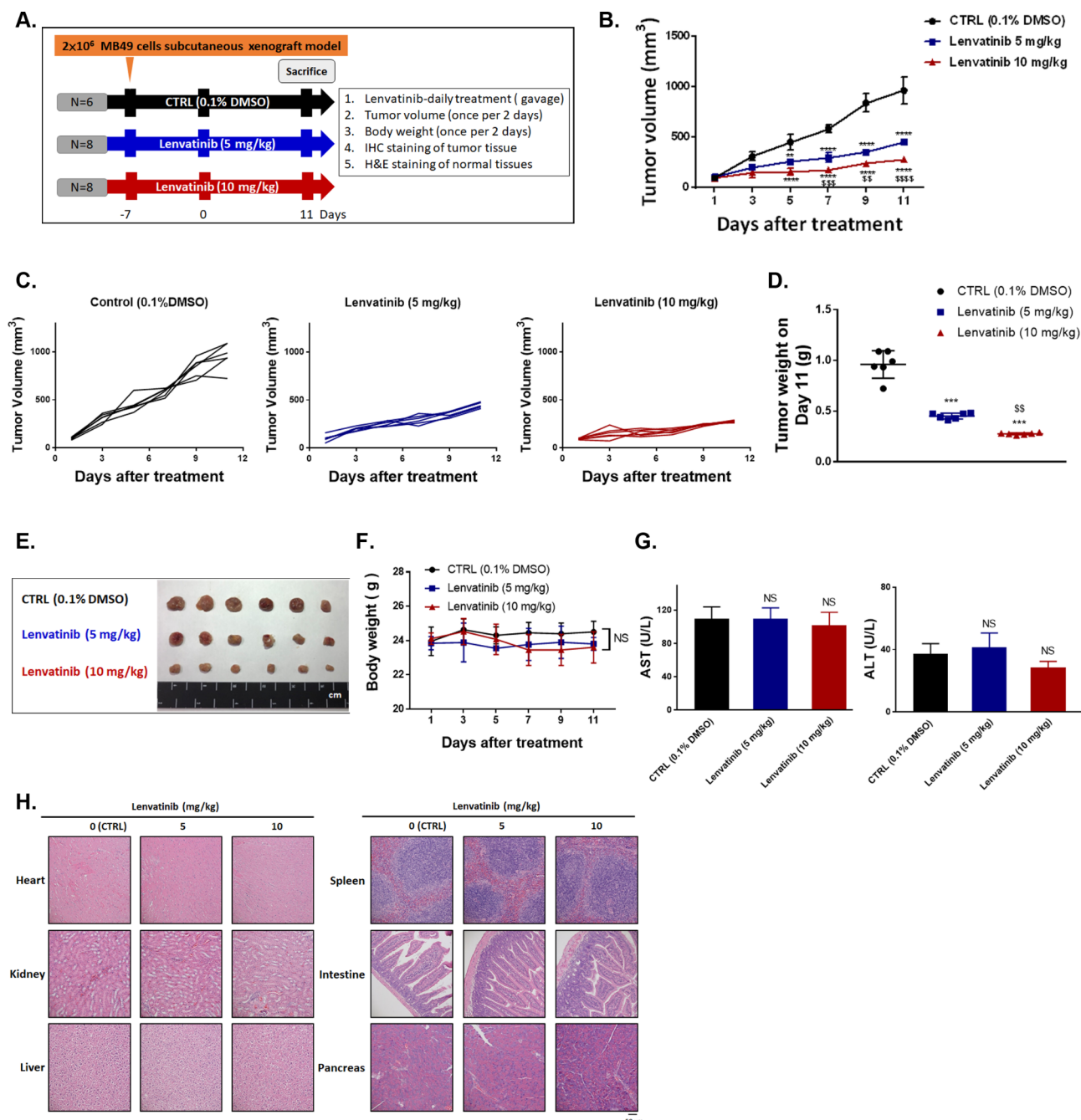


Fig. 4 Anti-BC efficacy of lenvatinib in an in vivo BC model. **(A)** The experimental flow chart depicting the treatment of MB-49 cells with lenvatinib is presented. **(B)** The average tumor size of each group and **(C)** the tumor progression in each mouse were recorded from day 0 to day 11 and displayed. **(D)** The weight of each extracted tumor was measured and presented. **(E)** Images of six representative tumors are displayed. **(F)** The body weight of each mouse, **(G)** biochemistry analysis of AST/ALT, and **(H)** tissue pathology of H&E staining from each group are presented. [(*, **) represent statistical significance with *P* values of less than 0.01 and 0.0005, respectively, compared to 0 μ M lenvatinib. (SS, SSS), represent statistical significance with *P* values of less than 0.01, 0.0005, and 0.0001 respectively, compared to 10 μ M lenvatinib. NS = no significant difference]

from undergoing apoptosis [39]. In addition to its inhibitory effects on anti-apoptotic proteins, our data revealed that treatment with lenvatinib resulted in a significant induction of apoptosis by activating both extrinsic and intrinsic pathways (Figs. 1C-J and 5A and C). Upregulation of N-cadherin and downregulation

of E-cadherin by EMT-related proteins, such as Twist, Snail, ZEB1, and ZEB2, lead to the breakdown of cellular adhesion and contribute to tumor metastasis [40, 41]. MMP9, as a gelatinase B, digests extracellular matrix (ECM) proteins, thereby enhancing tumor invasiveness and metastasis [42]. Positive Twist, Snail,

Table 3 Statistical analysis of tumor volume in different imipramine-treated groups and dates

Tukey's multiple comparisons test Lenvatinib	Mean difference	95.00% CI of difference	Summary	Adjusted PValue
Day 1				
0 vs. 5 mg/kg	-4.35	-75.78 to 67.08	ns	0.9885
0 vs. 10 mg/kg	1.967	-69.46 to 73.4	ns	0.9976
5 vs. 10 mg/kg	6.317	-65.11 to 77.75	ns	0.9758
Day 3				
0 vs. 5 mg/kg	109.9	38.45 to 181.3	**	0.0012
0 vs. 10 mg/kg	158.4	86.97 to 229.8	****	<0.0001
5 vs. 10 mg/kg	48.52	-22.91 to 119.9	ns	0.2431
Day 5				
0 vs. 5 mg/kg	196.7	125.2 to 268.1	****	<0.0001
0 vs. 10 mg/kg	293	221.6 to 364.4	****	<0.0001
5 vs. 10 mg/kg	96.33	24.9 to 167.8	**	0.0051
Day 7				
0 vs. 5 mg/kg	286.9	215.4 to 358.3	****	<0.0001
0 vs. 10 mg/kg	408.6	337.2 to 480.1	****	<0.0001
5 vs. 10 mg/kg	121.8	50.35 to 193.2	***	0.0003
Day 9				
0 vs. 5 mg/kg	487.7	416.2 to 559.1	****	<0.0001
0 vs. 10 mg/kg	599.1	527.7 to 670.6	****	<0.0001
5 vs. 10 mg/kg	111.5	40.04 to 182.9	**	0.0010
Day 11				
0 vs. 5 mg/kg	509.5	438.1 to 580.9	****	<0.0001
0 vs. 10 mg/kg	684.9	613.5 to 756.3	****	<0.0001
5 vs. 10 mg/kg	175.4	104 to 246.8	****	<0.0001

Table 4 Mean tumor growth time, delay time and inhibition rate in MB49 tumor-bearing mice after treatment with different doses of lenvatinib

Analysis methods	Lenvatinib		
	0 mg/kg	5 mg/kg	10 mg/kg
MTGT (day)*	6.35	15.63	30.08
MTGDT (day)#	na	9.28	23.73
MGIR [‡]	na	2.46	4.74

na: not available

*Mean tumor growth time (MTGT): the time at which the MB49 tumor volume reached 500 mm³. #Mean tumor growth delay time (MTGDT): the mean MB49 tumor growth time of the treated group minus that of the control group (0 mg/kg lenvatinib, 0.1% DMSO, CTRL). [‡]Mean growth inhibition rate (MGIR): the mean MB49 tumor growth time of the lenvatinib-treated group/the mean MB49 tumor growth time of the control group

Table 5 The biochemistry analysis of mouse serum from each treatment group is presented

Treatment option	Gamma Glutamyl Transpeptidase (γGT) value
Control (0.1% DMSO)	<3
Lenvatinib 5 mg/kg	<3
Lenvatinib 10 mg/kg	<3

and MMP9 expression is strongly associated with increased invasiveness, a higher risk of recurrence, and unfavorable outcomes in bladder cancer patients [43–45]. Constitutive activation of NF-κB promotes the induction of EMT-related proteins and MMP9 [42, 46]. Our data showed that lenvatinib effectively eliminated the expression of MMP9 and EMT-related proteins while inhibiting invasion (Figs. 3A-F and 5B, D and F).

In conclusion, our study has shown that lenvatinib induces apoptosis through both extrinsic and intrinsic

pathways and increases the sensitivity of bladder cancer cells to cisplatin. Additionally, lenvatinib disrupts EGFR/ERK/P38/NF-κB axis-mediated survival and metastatic potential. Based on our findings, we suggest lenvatinib as a potential therapeutic approach against bladder cancer, as it effectively promotes apoptosis and inhibits the EGFR/ERK/P38/NF-κB axis.

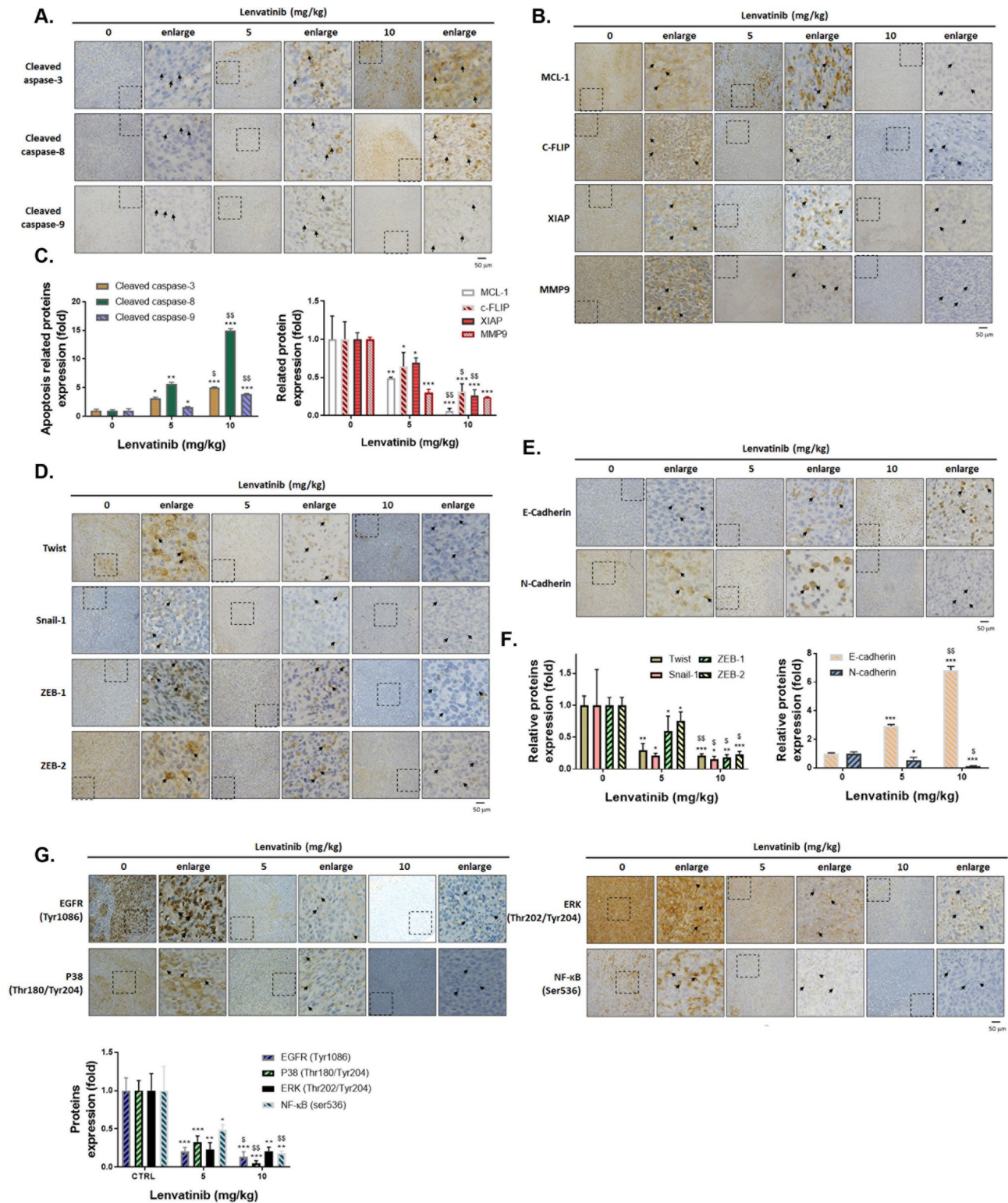


Fig. 5 Assessment of the anti-BC mechanism of lenvatinib in an in vivo BC model. (A-C) The protein expression levels associated with apoptosis and antiapoptosis in mouse tumor tissue are presented, along with their quantification results. (D-F) The protein expression levels associated with EMT regulation in mouse tumor tissue are presented, along with their quantification results. (G) The protein expression levels associated with EGFR-mediated signal transduction in mouse tumor tissue are presented, along with their quantification results. [(*, ***) represent statistical significance with P values of less than 0.05 and 0.0005, respectively, compared to 0 μM lenvatinib. (♯, ♯♯, ♯♯♯) represent statistical significance with a P value of less than 0.05, 0.01, and 0.0005 compared to 10 μM lenvatinib.]

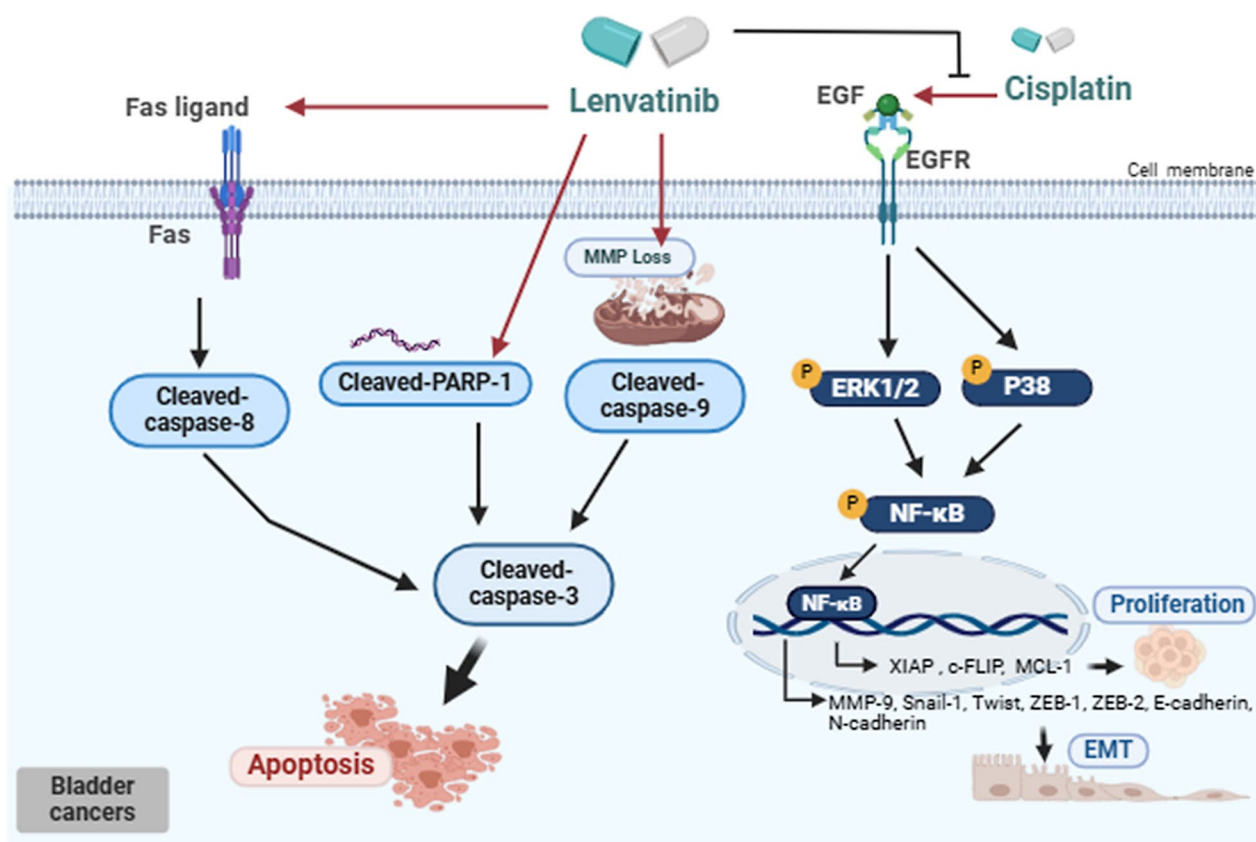


Fig. 6 The proposed mechanism of lenvatinib in combined with cisplatin. Lenvatinib demonstrated promising toxicity against bladder cancer (BC), enhanced the effect of cisplatin, and exhibited anti-tumor activity by inducing apoptosis, inhibiting metastasis, and modulating EGFR/ERK/P38/NF-κB signaling. These findings highlight the potential of lenvatinib as a therapeutic option for BC, either alone or in combination with existing treatments

Abbreviations

BC	Bladder cancer
NMIBC	Nonmuscle invasive bladder cancer
MIBC	Muscle invasive bladder cancer
EGFR	Epidermal growth factor receptor
EMT	Epithelial-mesenchymal transition
FGF	Fibroblast growth factor receptors
VEGF	Vascular endothelial growth factor receptors
MAPK	Mitogen-activated protein kinase
MCL-1	Myeloid cell leukemia-1
MMP9	Matrix metalloproteinase-9
XIAP	X-linked inhibitor of apoptosis protein
c-FLIP	Cellular FLICE-like inhibitory protein

Supplementary Information

The online version contains supplementary material available at <https://doi.org/10.1186/s12935-024-03597-7>.

Supplementary Material 1

Acknowledgements

Experiments and data analysis were performed in part through the use of the Medical Research Core Facilities Center, Office of Research & Development at China Medical University, Taichung, Taiwan, ROC.

Author contributions

CH Chiang, JD Yang, WL Liu and FY Chang performed experiments, analyzed data and wrote the draft of manuscript. CH Chiang, JD Yang, WL Liu, FY Chang

and CJ Yang analyzed the data. CH Chiang, KW Hsu, IT Chiang and FT Hsu conceived the ideas, oversaw the research and wrote the final version of the manuscript. KW Hsu, IT Chiang, and FT Hsu prepared the revised version of the manuscript.

Funding

This study was supported by Show-Chwan Memorial Hospital, Changhua, Taiwan, R.O.C. (ID: SRD-108008), Chang Bing Show Chwan Memorial Hospital, Changhua, Taiwan, R.O.C. (ID: BRD-108027), Ministry of Science and Technology (MOST), Taipei, Taiwan, R.O.C. (ID: MOST 111-2314-B-019-001-MY3), National Yang Ming Chiao Tung University Hospital, Yilan, Taiwan, R.O.C. (ID: RD2021-007) and China Medical University, Taichung, Taiwan (ID: CMU113-MF-61). This work was also financially supported by the "Drug Development Center, China Medical University" from The Featured Areas Research Center Program within the framework of the Higher Education Sprout Project by the Ministry of Education (MOE) in Taiwan.

Data availability

The supporting data that underpin the findings of this study are available upon request from the corresponding author.

Declarations

The authors have reported no potential competing interests.

Studies involving animal subjects

The animal study conducted in this research was subjected to review and approval by the Institutional Animal Care and Use Committee (IACUC) at China Medical University, Taichung, Taiwan (ID: CMU-IACUC-2023-051).

Ethics and Consent to participate declarations

not applicable.

Author details

¹Division of Urology, Department of Surgery and Department of Research and Development, Taoyuan General Hospital, Ministry of Health and Welfare, Taoyuan, Taiwan, R.O.C.

²Department of Urology, National Taiwan University Hospital, Taipei, Taiwan, R.O.C.

³Department and Institute of Pharmacology, School of Medicine, National Yang Ming Chiao Tung University, Taipei, Taiwan, R.O.C.

⁴Division of Urology, Department of Surgery, National Yang-Ming Chiao Tung University Hospital, Yilan, Taiwan, R.O.C.

⁵Department of Radiation Oncology, Show Chwan Memorial Hospital, Changhua, Taiwan, R.O.C.

⁶Department of Biological Science and Technology, China Medical University, Office: 7F, Research building, No. 100, Jingmao 1st Rd., Beitun Dist, Taichung City 406040, Taiwan, R.O.C.

⁷Division of Urology, Department of Surgery, Chang Bing Show-Chwan Memorial Hospital, Changhua, Taiwan, R.O.C.

⁸Research Center for Cancer Biology, China Medical University, Taichung, Taiwan, R.O.C.

⁹Drug Development Center, Program for Cancer Biology and Drug Discovery, China Medical University, Taichung, Taiwan, R.O.C.

¹⁰Institute of Translational Medicine and New Drug Development, China Medical University, Taichung, Taiwan, R.O.C.

¹¹Department of Radiation Oncology, Chang Bing Show Chwan Memorial Hospital, Lukang, Taiwan, R.O.C.

¹²Department of Medical Imaging and Radiologic Sciences, Central Taiwan University of Science and Technology, Taichung, Taiwan, R.O.C.

¹³Medical Administrative Center, Show Chwan Memorial Hospital, Changhua, Taiwan, R.O.C.

¹⁴Department of Life Sciences, National Central University, Taoyuan, Taiwan, R.O.C.

Received: 26 October 2023 / Accepted: 3 December 2024

Published online: 15 February 2025

References

1. Tsai TF, Chen PC, Lin YC, Chou KY, Chen HE, Ho CY, Lin JF, Hwang TI. Benzyl isothiocyanate promotes miR-99a expression through ERK/AP-1-dependent pathway in bladder cancer cells. *Environ Toxicol.* 2020;35(1):47–54.
2. Hu X, Li G, Wu S. Advances in diagnosis and therapy for bladder Cancer. *Cancers (Basel)* 2022, 14(13).
3. Chamie K, Litwin MS, Bassett JC, Daskivich TJ, Lai J, Hanley JM, Konety BR, Saitgal CS. Recurrence of high-risk bladder cancer: a population-based analysis. *Cancer.* 2013;119(17):3219–27.
4. Li W, Wang Y, Tan S, Rao Q, Zhu T, Huang G, Li Z, Liu G. Overexpression of Epidermal Growth Factor Receptor (EGFR) and HER-2 in Bladder Carcinoma and its Association with patients' clinical features. *Med Sci Monit.* 2018;24:7178–85.
5. Uribe ML, Marrocco I, Yarden Y. EGFR in Cancer: signaling mechanisms, drugs, and Acquired Resistance. *Cancers (Basel)* 2021, 13(11).
6. Hashimoto M, Fujita K, Tomiyama E, Fujimoto S, Adomi S, Banno E, Minami T, Takao T, Nozawa M, Fushimi H, et al. Immunohistochemical analysis of HER2, EGFR, and Nectin-4 expression in Upper urinary tract Urothelial Carcinoma. *Anticancer Res.* 2023;43(1):167–74.
7. Rebouissou S, Bernard-Pierrot I, de Reyniès A, Lepage ML, Krucker C, Chapeaublanc E, Héroult A, Kamoun A, Caillaud A, Letouzé E, et al. EGFR as a potential therapeutic target for a subset of muscle-invasive bladder cancers presenting a basal-like phenotype. *Sci Transl Med.* 2014;6(244):244ra291.
8. Tsai YC, Ho PY, Tzen KY, Tuan TF, Liu WL, Cheng AL, Pu YS, Cheng JC. Synergistic blockade of EGFR and HER2 by New-Generation EGFR tyrosine kinase inhibitor enhances Radiation Effect in bladder Cancer cells. *Mol Cancer Ther.* 2015;14(3):810–20.
9. Mooso BA, Vinnall RL, Mudryj M, Yap SA, deVere White RW, Ghosh PM. The role of EGFR family inhibitors in muscle invasive bladder cancer: a review of clinical data and molecular evidence. *J Urol.* 2015;193(1):19–29.
10. Vavrová K, Indra R, Pompach P, Heger Z, Hodek P. The impact of individual human cytochrome P450 enzymes on oxidative metabolism of anticancer drug lenvatinib. *Biomed Pharmacother.* 2022;145:112391.
11. Liu YC, Huang BH, Chung JG, Liu WL, Hsu FT, Lin SS. Lenvatinib inhibits AKT/NF- κ B signaling and induces apoptosis through Extrinsic/Intrinsic pathways in Non-small Cell Lung Cancer. *Anticancer Res.* 2021;41(1):123–30.
12. Wu CH, Hsu FT, Chao TL, Lee YH, Kuo YC. Revealing the suppressive role of protein kinase C delta and P38 mitogen-activated protein kinase (MAPK)/NF- κ B axis associates with lenvatinib-inhibited progression in hepatocellular carcinoma in vitro and in vivo. *Biomed Pharmacother.* 2022;145:112437.
13. Du G, Hao C, Gu Y, Wang Z, Jiang WG, He J, Cheng S. A novel NHERF1 mutation in human breast Cancer inactivates inhibition by NHERF1 protein in EGFR Signaling. *Anticancer Res.* 2016;36(3):1165–73.
14. Yueh PF, Lee YH, Chiang IT, Chen WT, Lan KL, Chen CH, Hsu FT. Suppression of EGFR/PKC- δ /NF- κ B signaling Associated with imipramine-inhibited progression of Non-small Cell Lung Cancer. *Front Oncol.* 2021;11:735183.
15. Jiang W, Tian W, Ijaz M, Wang F. Inhibition of EGF-induced migration and invasion by sulfated polysaccharide of *Sepiella maindroni* ink via the suppression of EGFR/Akt/P38 MAPK/MMP-2 signaling pathway in KB cells. *Biomed Pharmacother.* 2017;95:95–102.
16. Chen J-H, Chiang I-T, Hsu F-T. Protein kinase B inactivation is Associated with Magnolol-enhanced therapeutic efficacy of Sorafenib in Hepatocellular Carcinoma in Vitro and in vivo. *Cancers.* 2020;12(1):87.
17. Chen WT, Chen CH, Su HT, Yueh PF, Hsu FT, Chiang IT. Amentoflavone induces cell-cycle arrest, apoptosis, and Invasion Inhibition in Non-small Cell Lung Cancer cells. *Anticancer Res.* 2021;41(3):1357–64.
18. Chen JC, Chuang HY, Liao YJ, Hsu FT, Chen YC, Wang WH, Hwang JJ. Enhanced cytotoxicity of human hepatocellular carcinoma cells following pretreatment with sorafenib combined with trichostatin A. *Oncol Lett.* 2019;17(1):638–45.
19. Chiang CH, Chung JG, Hsu FT. Regorafenib induces extrinsic/intrinsic apoptosis and inhibits MAPK/NF- κ B-modulated tumor progression in bladder cancer in vitro and in vivo. *Environ Toxicol.* 2019;34(6):679–88.
20. Chen WT, Chen YK, Lin SS, Hsu FT. Hyperforin suppresses Tumor Growth and NF- κ B-mediated anti-apoptotic and invasive potential of non-small cell Lung Cancer. *Anticancer Res.* 2018;38(4):2161–7.
21. Chen CH, Huang YC, Lee YH, Tan ZL, Tsai CJ, Chuang YC, Tu HF, Liu TC, Hsu FT. Anticancer efficacy and mechanism of Amentoflavone for sensitizing oral squamous cell carcinoma to Cisplatin. *Anticancer Res.* 2020;40(12):6723–32.
22. Hsu FT, Sun CC, Wu CH, Lee YJ, Chiang CH, Wang WS. Regorafenib induces apoptosis and inhibits metastatic potential of human bladder carcinoma cells. *Anticancer Res.* 2017;37(9):4919–26.
23. Lin CH, Lin KH, Ku HJ, Lee KC, Lin SS, Hsu FT. Amentoflavone induces caspase-dependent/independent apoptosis and dysregulates cyclin-dependent kinase-mediated cell cycle in colorectal cancer in vitro and in vivo. *Environ Toxicol.* 2023;38(5):1078–89.
24. Chen CH, Hsu FT, Chen WL, Chen JH. Induction of Apoptosis, Inhibition of MCL-1, and VEGF-A Expression Are Associated with the Anti-Cancer Efficacy of Magnolol Combined with Regorafenib in Hepatocellular Carcinoma. *Cancers (Basel)* 2021, 13(9).
25. Chiang CH, Yeh CY, Chung JG, Chiang IT, Hsu FT. Amentoflavone induces apoptosis and reduces expression of anti-apoptotic and metastasis-associated proteins in bladder Cancer. *Anticancer Res.* 2019;39(7):3641–9.
26. Yang CJ, Tan ZL, Yang JD, Hsu FT, Chiang CH. Fluoxetine inactivates STAT3/NF- κ B signaling and promotes sensitivity to cisplatin in bladder cancer. *Biomed Pharmacother.* 2023;164:114962.
27. Liu YC, Lin CH, Chen KT, Lai DW, Hsu FT. Inactivation of EGFR/ERK/NF- κ B signalling associates with radiosensitizing effect of 18 β -glycyrrhetic acid on progression of hepatocellular carcinoma. *J Cell Mol Med.* 2023;27(11):1539–49.
28. Gontero P, Banisadr S, Frea B, Brausi M. Metastasis markers in bladder Cancer: a review of the literature and clinical considerations. *Eur Urol.* 2004;46(3):296–311.
29. Mittal V. Epithelial mesenchymal transition in Tumor Metastasis. *Annu Rev Pathol.* 2018;13:395–412.
30. Wolf P. Inhibitor of apoptosis proteins as therapeutic targets in bladder cancer. *Front Oncol* 2023, 13.
31. Hashmi AA, Hussain ZF, Irfan M, Khan EY, Faridi N, Naqvi H, Khan A, Edhi MM. Prognostic significance of epidermal growth factor receptor (EGFR) over expression in urothelial carcinoma of urinary bladder. *BMC Urol.* 2018;18(1):59.

32. Liu YC, Tsai JJ, Weng YS, Hsu FT. Regorafenib suppresses epidermal growth factor receptor signaling-modulated progression of colorectal cancer. *Biomed Pharmacother*. 2020;128:110319.
33. Mhone TG, Chen MC, Kuo CH, Shih TC, Yeh CM, Wang TF, Chen RJ, Chang YC, Kuo WW, Huang CY. Daidzein Synergizes with Gefitinib to induce ROS/JNK/c-Jun activation and inhibit EGFR-STAT/AKT/ERK pathways to enhance lung adenocarcinoma cells chemosensitivity. *Int J Biol Sci*. 2022;18(9):3636–52.
34. Hua F, Hao W, Wang L, Li S. Linear Ubiquitination mediates EGFR-Induced NF- κ B pathway and Tumor Development. *Int J Mol Sci* 2021, 22(21).
35. Lee SJ, Park SS, Lee US, Kim WJ, Moon SK. Signaling pathway for TNF- α -induced MMP-9 expression: mediation through P38 MAP kinase, and inhibition by anti-cancer molecule magnolol in human urinary bladder cancer 5637 cells. *Int Immunopharmacol*. 2008;8(13–14):1821–6.
36. Chen SY, Chao CN, Huang HY, Zhao PW, Fang CY. Artesunate exhibits Synergy with cisplatin and cytotoxicity for Upper Tract and bladder urothelial carcinoma cells. *Anticancer Res*. 2023;43(3):1175–84.
37. Xing J, Chen W, Chen K, Zhu S, Lin F, Qi Y, Zhang Y, Han S, Rao T, Ruan Y et al. TFAP2C Knockdown Sensitizes Bladder Cancer Cells to Cisplatin Treatment via Regulation of EGFR and NF- κ B. *Cancers (Basel)* 2022, 14(19).
38. Chiang IT, Chen WT, Tseng CW, Chen YC, Kuo YC, Chen BJ, Weng MC, Lin HJ, Wang WS. Hyperforin inhibits cell growth by inducing intrinsic and extrinsic apoptotic pathways in Hepatocellular Carcinoma cells. *Anticancer Res*. 2017;37(1):161–7.
39. Pfeffer CM, Singh ATK. Apoptosis: a target for Anticancer Therapy. *Int J Mol Sci* 2018, 19(2).
40. Ghulam J, Stuerken C, Wicklein D, Pries R, Wollenberg B, Schumacher U. Immunohistochemical Analysis of Transcription Factors and markers of epithelial-mesenchymal transition (EMT) in human tumors. *Anticancer Res*. 2019;39(10):5437–48.
41. Cao R, Yuan L, Ma B, Wang G, Qiu W, Tian Y. An EMT-related gene signature for the prognosis of human bladder cancer. *J Cell Mol Med*. 2020;24(1):605–17.
42. Pan PJ, Tsai JJ, Liu YC. Amentoflavone inhibits metastatic potential through suppression of ERK/NF- κ B activation in Osteosarcoma U2OS cells. *Anticancer Res*. 2017;37(9):4911–8.
43. Gou Y, Ding W, Xu K, Wang H, Chen Z, Tan J, Xia G, Ding Q. Snail is an independent prognostic indicator for predicting recurrence and progression in non-muscle-invasive bladder cancer. *Int Urol Nephrol*. 2015;47(2):289–93.
44. Fondreville ME, Kantelip B, Reiter RE, Chopin DK, Thiery JP, Monnien F, Bittard H, Wallerand H. The expression of twist has an impact on survival in human bladder cancer and is influenced by the smoking status. *Urol Oncol*. 2009;27(3):268–76.
45. Reis ST, Leite KR, Piovesan LF, Pontes-Junior J, Viana NI, Abe DK, Crippa A, Moura CM, Adonias SP, Srougi M, et al. Increased expression of MMP-9 and IL-8 are correlated with poor prognosis of bladder Cancer. *BMC Urol*. 2012;12:18.
46. Xia Y, Shen S, Verma IM. NF- κ B, an active player in human cancers. *Cancer Immunol Res*. 2014;2(9):823–30.

Publisher's note

Springer Nature remains neutral with regard to jurisdictional claims in published maps and institutional affiliations.